Feasibility Study of a Modular Multi-Purpose Frigate with an Integrated Power & Energy System

Luca Braidotti
Dept. of Engineering and Architecture
University of Trieste
Trieste, Italy
lbraidotti@units.it

Andrea Vicenzutti
Dept. of Engineering and Architecture
University of Trieste
Trieste, Italy
avicenzutti@units.it

Daniele Bosich
Dept. of Engineering and Architecture
University of Trieste
Trieste, Italy
dbosich@units.it

Vittorio Bucci
Dept.of Engineering and Architecture
University of Trieste
Trieste, Italy
vbucci@units.it

Giorgio Sulligoi
Dept.of Engineering and Architecture
University of Trieste
Trieste, Italy
gsulligoi@units.it

Giorgio Trincas
Dept. of Engineering and Architecture
University of Trieste
Trieste, Italy
trincas@units.it

***Abstract*— This paper presents a feasibility study of a modular multi-purpose frigate with an integrated power and energy system (IPES) and a Combined Diesel Electric and Gas (CODLAG) propulsion system. The modular design offers greater flexibility, enabling the vessel to perform a wider range of missions thanks to innovative hull form and a large capacity for carrying a containerized payload. The study evaluates also the feasibility and potential benefits of two possible configurations for the Energy Storage System (ESS) integration in the onboard IPES, enabled by the specific ship design. The utilization of peak shaving technology reliying on supercapacitors has a limited impact on the ship in terms of weight and volume, thus being the most appropriate solution for CODLAG frigates. Conversely, Li-ion batteries can enable zero-emission mode. A large ESS capacity can be integrated onboard in the available weight and volume margins (enabled by the specific ship design), aimed at improving energy efficiency in port, manoeuver, and combat modes (by avoiding non-optimal load rates on generators).**

***Index Terms*-- Modular design, Integrated power energy system, Added resistance, Peak shaving, Naval ship, Frigate**

I. Introduction

In recent years, navies around the world have been investing heavily in larger and more capable frigates to meet the increasingly complex demands of modern maritime operations [1]. These vessels must be able to carry out a wide range of missions, including anti-submarine warfare, air defence, and maritime interdiction, while also being versatile enough to adapt to emerging threats and changing operational environments.

In such context, modular design has become an increasingly popular approach for designing all kinds of naval ships due to its ability to improve the adaptability, flexibility, and sustainability of naval platforms [3]. In particular, the containerization of modules has emerged as a key trend in the modular design of naval ships, offering numerous benefits over traditional shipbuilding methods. The main advantages of mission modularity are decoupling between platform and plants, greater redundancy, easier repairs, maintenance and overhauls, simple refitting, and plants' upgrade. Moreover, the number of crew members can be adapted to the specific mission. Containerized modules are pre-fabricated and pre-equipped units that can be easily transported, installed, and replaced as needed, providing a high degree of customization and flexibility to the ship's configuration [4]. This approach also enables more efficient maintenance and repair processes, reducing downtime and increasing operational readiness [5]. Moreover, containerization can facilitate the integration of new technologies and capabilities, enhancing the ship's overall mission effectiveness [6].

As frigates have grown in size and complexity [7], the need for an efficient and effective power and energy system has become more important than ever. The integrated power and energy system (IPES) is a new approach to naval ship design that combines multiple energy sources, including gas turbines, diesel generators, and batteries, to provide the necessary power and flexibility for modern frigates [9]. IPES has the potential to not only improve the operational capabilities of naval ships, but also to reduce their environmental footprint through increased efficiency and reduced fuel consumption [10]. This is an important consideration as the global community becomes increasingly concerned about reducing greenhouse gas emissions and minimizing the impact of human activities on the environment [11].

TABLE I. INITIAL DESIGN REQUIREMENTS

Main dimensions	L_{OA} < 150.00 m
	B_{max} < 21.00 m
	T_{max} < 6.00 m
Full load displacement	Δ ≈ 8,000 t
Operating speeds (PEM)	V = 12 kn in SS6, BF 7
	V = 15 kn in SS6, BF 7
	V = 18 kn in SS4, BF 5 - 18 months roughness
Combat speed	V = 20 kn on sea trials
Maximum speed	V = 28.5 kn on sea trials on Gas Turbine
	V = 29.5 kn on sea trials (CODLAG)
	V = 28 kn at the end of life on Gas Turbine
Range	8,000 nm
Seakeeping	STANAG 4154 Criteria
Manoeuvering	RinaMil rules
Radar cross section	Minimize

TABLE II. MAIN CHARACTERISTICS OF THE FRIGATE

Particulars	Symbols	Value
Length overall	L_{OA}	148.80 m
Length at waterline	L_{WL}	147.25
Beam, maximum	B_{max}	18.90 m
Beam, at waterline	B	17.86 m
Draft	T	5.68 m
Block coefficient	C_B	0.521
Deadweight	DWT	1708 t
Maximum propulsion power	P_{max}	44.000 kW

This paper presents a feasibility study of a modular multi-purpose frigate that exploits an IPES and a COmbined Diesel eLectric And Gas (CODLAG) propulsion system. In detail, the main objective is to define a new ship concept with innovative hull forms (X-bow) and a large capacity for carrying a containerized payload. Besides, this work aims to evaluate the feasibility and potential benefits coming to two configurations of the onboard IPES (for peak shaving and for enabling zero-emission mode), exploiting the available weight and volume margins enabled by the ship design. The targets are then multiple, including increased efficiency, reduced fuel consumption, and improved operational flexibility.

II. FRIGATE MODULAR DESIGN

A. Design requirements

The twin-screw frigate shall have a CODLAG propulsion system with two reversible electric motors capable to absorb 4 MW. Four diesel generators, each one of 3.1 MW, drive the electric motors and provide the other electric loads. The gas turbine has a power of 36 MW and is connected to the electric motors through a reduction gear. A retractable azimuth thruster shall be fitted, with a minimum power of 1 MW, to guarantee the minimum speed of 12 knots (auxiliary propulsion) and to assist in mooring maneuvers (power thruster). Table I summarizes the primary requirements to be met from the early stages of the prototype vessel design. The displacement is assumed to increase by 6% at the end of life.

B. Selection of the frigate prototype

A multiattribute decision-making procedure (set-based design approach) has been employed to select the 'best possible' frigate among a set of non-dominated designs belonging to the Pareto-frontier [12-14]. The main particulars of the best-possible ship extracted from the frontier are given in Table II. The ship is equipped with a set of fixed weapons and sensors. In detail, concerning weapons, the ship's main fixed armament includes a 127/64 gun, a 76/62 gun, 32-cell A50 Vertical Launching System (VLS). The combat system is complemented by a complete set of sensors and electronic systems, including a fully digital Active Electronically Scanned Array (AESA) multifunction radar (S-band), two extra long-range naval optronic identification & fire control systems, an integrated digital communication system, and an advanced digital electronic warfare system. The ship is fitted with a flight deck and two hangars for two medium-sized helicopters. Finally, the ship in standard configuration can accommodate a total of 145 personnel: 16 officers, 23 petty officers, and 106 sailors. The frigate can accommodate a modular payload (that will be thoroughly described in Section II.C) and has a reserve of space/payload for the installation of additional systems in the forebody up to 130 t and 600 m^3 (available margin).

C. Modular spaces

Recent advances in the containerization of modules for warships have focused on improving the design and construction of modular units, as well as developing new standards and regulations to ensure compatibility and interoperability between different modules and platforms. Some notable examples include the use of advanced materials and manufacturing techniques, such as 3D printing and composite materials, to enhance the performance and durability of modules [15-18].

Another important aspect of containerization is the use of common interfaces and connectors, such as the NATO Generic Open Architecture (NGOA), to enable the seamless integration of modules from different suppliers and countries [19]. This approach has been successfully implemented in several naval programs, such as the Danish StanFlex system and the US Navy's Modular Mission Payload (MMP) concept [20-22].

Containerization of modules has become an integral part of modern warship design, providing a flexible and adaptable platform for naval operations [23]. Ongoing research and development in this area are likely to further improve the capabilities and effectiveness of containerized modules in future naval programs [24-26].

In this framework and to fulfill the design requirements, in the proposed design the containerization paradigm has been extensively applied. Fig. 1 highlights the modular spaces on the ship's general arrangement plan. It can be noted that, compared to other existing frigates, the proposed design differs in terms of the volumetric compactness of the central spaces above the main deck, where most of the modules can be installed. In detail, besides the above-mentioned fixed equipment, the frigate can allocate on a stern ramp one 40 ft module (for a large assault Rigid Hull Inflatable Boat (RHIB) or towed array sonar). In the superstructure center (on three decks), up to 18 small (20 ft) and 4 large (40 ft) containerized modules can be stowed having an overall weight of up to 300 t. These modules enable complete customization of the frigate for a specific mission. For instance, they can add additional weapon systems (e.g. gun turret, torpedos, VLS), accommodations (e.g. cabins, command center, armory, hospital center), vehicles (e.g.

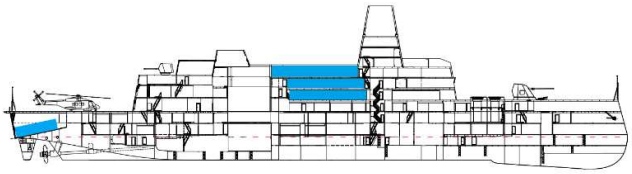

Figure 1. Profile view highlighting the modular spaces

Figure 2. Rendering of the prototype

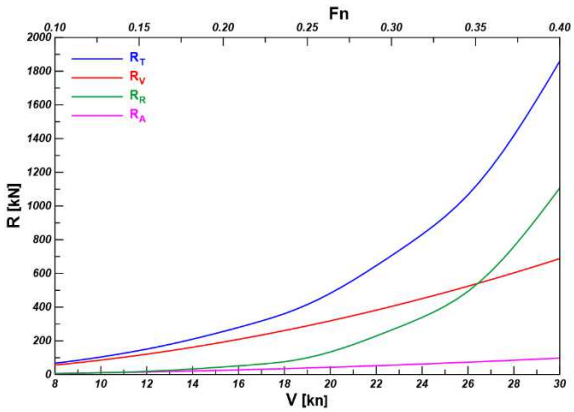

Figure 3. Total resistance and resistance components in calm water

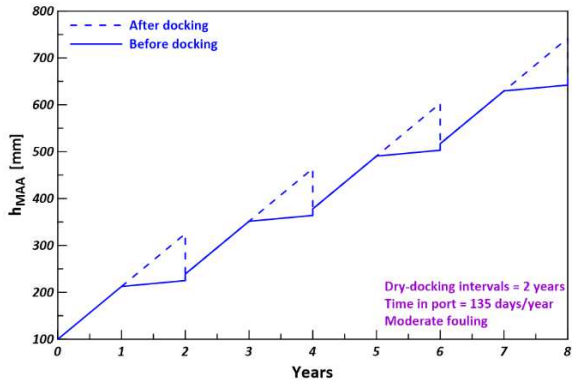

Figure 4. Time history of hull roughness

RHIBs, submarines, unmanned surface/underwater/aerial vehicles) or to extend the ship capabilities (e.g. additional generator units, batteries, workshops, special equipment). All the modules employ standard plug-in interfaces as needed (electricity, compressed air, oil, onboard network) and can be loaded and moved near the ship side, even during navigation for launching or warfare operations. This is done through 4 large closable hatches on the ship side. Modules mounted on the higher deck can also utilize a hatch on the open deck (e.g. for missile launching). Fig. 2 shows an isometric view from the forebody of the frigate prototype characterized by a new variant of the X-bow concept.

III. Hydrodynamic Assessment

In the set-based design selection process, a set of critical hydrodynamic items have been taken into account to be numerically sure that the ship performs well and meets the design requirements. Some of these items are as follows:

- low resistance behavior
- high propulsive power and fuel efficiency
- good seakeeping ability (motions, accelerations, *MSI*, *MII*)
- good manoeuvrability (course stability, turning circle, zig-zag manoeuvre)

Particular attention was paid to seakeeping performance: design for seakeeping was the golden rule in selecting the hull form. In particular, the bow flare was limited as much as possible to avoid high-wave induced impacts, whipping vibrations and involuntary speed loss.

A. Resistance

a) Calm water resistance

The calm water resistance was rated with an in-house-built code where the residual resistance component is assessed via a set of distinct formulas according to the Froude number.

Beyond the total resistance R_T, Fig. 3 shows the viscous resistance R_V, the residual resistance R_R and the added resistance due to appendages and air.

b) Hull roughness

Since an estimate of the increase in hull resistance is required in the specification during the service speed, the effect of hull roughness was summed up to the calm water resistance. The average roughness from the accumulation of fouling was expressed by Malone et al. [27]. Here the frigate is assumed to be dry-docked at intervals of two years. The increase in the hull roughness is assumed to be 14 μm per docking. The hull roughness h_{MAA} for each dry-docking is given in the time-history diagram of dry-docking intervals which includes roughness due to corrosion, as depicted in Fig. 4.

c) Added Resistance in Waves

As mentioned in Table I, the design requirements included operability in harsh sea conditions. Hence, it is necessary to assess the added resistance of the ship in a seaway. Here, the computation has been carried out in the time domain with the following procedure.

The added resistance R_{AW} in irregular waves can be computed using a spectral approach [28]. When associated with a single regular wave, it can be expressed as:

$$\delta R_{AW} = 2C_{AW}(\omega_e)S_\zeta(\omega_e)\delta\omega_e \quad (1)$$

where ω_e is the encounter frequency, $S_\zeta(\omega_e)$ is the wave spectrum (here the Pierson-Moskowitz spectrum has been used to model the irregular sea [29]) and C_{AW} is a dimensional added resistance response function defined as:

$$C_{AW}(\omega_e) = \frac{R_W(\omega_e)}{\zeta_a^2} \quad (2)$$

where ζ_a is the regular wave amplitude. In the present work, the response function has been evaluated with a statistical method in head-sea condition [30]. The mean value of the resistance is assessed as:

$$\bar{R}_{AW} = 2\int_0^\infty C_{AW} S_\zeta(\omega_e) d\omega_e \quad (3)$$

A time record can be then generated as a sum of the single components assuming a small frequency interval (here $\delta\omega_e$ = 0.001 rad/s has been adopted) as:

$$R_{AW}(t) = \bar{R}_{AW} + \sum_{i=0}^{N} a_i \cos(\omega_{e_i} t + \varphi_i) \quad (4)$$

where φ_i is the random phase related to the i-th considered encounter frequency ω_{e_i} and a_i is defined as:

$$a_i = \sqrt{2 C_{AW}(\omega_{e_i}) S_\zeta(\omega_e) \delta\omega_e} \quad (5)$$

The time record obtained at a speed of 16 kn in Sea State (SS) 5 (T_z = 7.5 s, $H_{1/3}$ = 3.25 m) is provided in Fig. 5.

d) Total service resistance

Once the added resistance due to waves and roughness are assessed, they are added to the resistance in calm water and to the wind resistance, evaluated according to the metamodels provided by Fujiwara and Nomura [31]. The resistance values in calm water and in given environmental conditions are given in Table III.

B. Powering Performance

The added resistance due to a seaway and roughness was here represented by the addition of power to sustain the speed. Loss in propulsive efficiency due to many factors (ship motions, wind load, wave reflection, roughness on propellers, overloading, and emergence of the propellers) was considered too. The average values of the open-water propeller characteristics have been slightly reduced compared to the calm-water ones because of the change in propeller loading due to the resistance increase. Since resistance tests and self-propulsion tests experiments on some destroyer has shown that the wake fraction is almost the same as in calm water except in the slow speed range, and the thrust deduction factor in waves is slightly higher in waves than in still water, the propulsive coefficients of the frigate are assumed to be the same in waves as in calm water [32].

Fig. 6 shows the trend of the power demand curves of the propellers in different service conditions, where the two electric motors are expected to suffice. All the operating speeds achievable with the diesel-electric propulsion system alone satisfy the design requirements. In particular, in calm water, the achievable speed is higher than 20 knots, while the transit speed of 18 knots in SS4 with roughness on the hull and propellers is more than satisfactory. As to operations in SS6, there is no problem to achieve the required speeds.

Fig. 7 shows the propellers' load curves simulating the sea trials of the new-build frigate and the ship's end-of-life displacement with hull roughness at 18 months in both gas turbine (shaft power P_S = 36 MW) and CODLAG modes (P_S = 44 MW). Even at high speeds, the requirements are largely satisfied.

TABLE III. RESISTANCE IN REQUIRED SERVICE CONDITIONS

Case	Service Condition	Calm Water Resistance	Total Service Resistance
A	Speed of 12 kn, SS6, BF 7	150.1 kN	286.3 kN
B	Speed of 15 kn, SS6, BF 7	240.5 kN	463.8 kN
C	Speed of 18 kn, SS4, BF 5	344.4 kN	475.5 kN
D	Speed of 20 kn, calm water	440.6 kN	440.6 kN
E	Speed of 28 kn, calm water	1372.4 kN	1372.4 kN
F	Speed of 29.5 kn, calm water	1731.7 kN	1731.7 kN

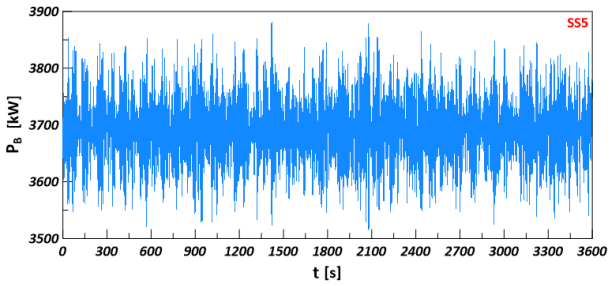

Figure 5. Time record of single-axis brake power in SS5 at V = 16 kn

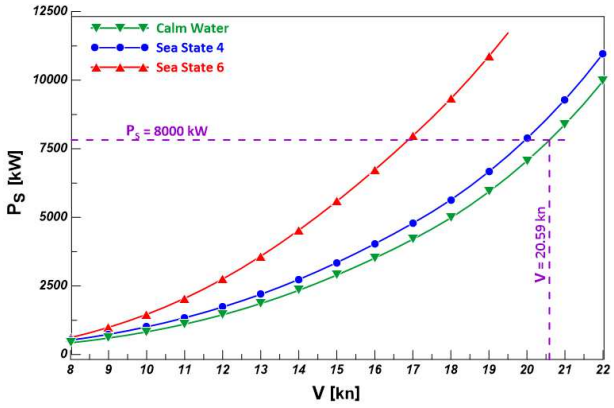

Figure 6. Electric motors' power demand in diesel-electric mode

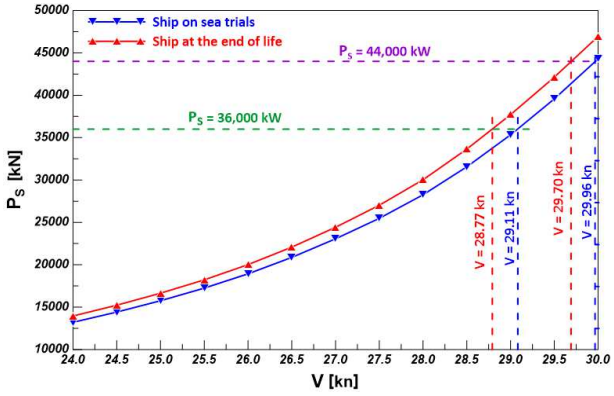

Figure 7. Eletric motors' power demand in TAG and CODLAG modes

IV. INTEGRATED POWER & ENERGY SYSTEM

A. Power system layout and components

The ship's IPES is depicted in Fig. 8. The radial architecture uses two main high voltage (HV) busbars, operating at 6.6 kV, powered by two 3.1 MW Diesel Generators (DGs) each. The variable speed drives of the electric propulsion motors (EMs) are connected to the HV buses, which supply also the 6.6/0.4 kV transformers feeding the LV loads, one azimuthal propeller used for maneuvering, and one HV shore panel. The latter supplies the ship from the shore at berth using a high-voltage shore connection. The ship is endowed with a second shore connection, which directly supplies the LV busbars. As stated in the design requirements, the two EMs are 4 MW each, which can be used as shaft generators also thanks to their active front-end drives. Finally, a single 36 MW gas turbine (GT) can be also used to power the propulsion, through a dedicated gearbox.

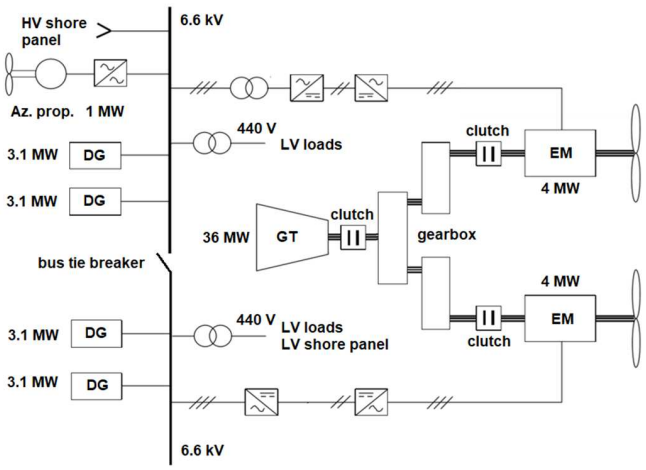

Figure 8. Ship's Integrated Power and Energy System.

In the Fig. 8 architecture, also the installation of Energy Storage Systems (ESSs) is foreseeable. They are not shown for the sake of simplicity. The ESSs scope and sizing is discussed in the following subsections, as well as the specific location of their interface to the power system.

B. Electric load balance

The power is calculated on the low voltage side of the IPES. At this point, all the loads are connected, whereas the propulsion is modeled as the total equivalent electrical load in a given Operative Condition (OC). The high voltage side load without propulsion is then calculated using transformers' efficiency to obtain the equivalent low voltage electrical load, and adding the azimuthal propeller load in the relevant OCs (i.e., "preparation for sea", where the maneuvering for entering/exiting the port is considered). By adding the propulsion power obtained by means of the Section III load/power curve, and applying an additional 10% design

TABLE IV. ELECTRIC LOADS BALANCE

OC	At berth		Prep. for sea		Cruise at 12 kn SS6 BF 7		Cruise at 15 kn SS6 BF 7		Cruise at 18 kn SS4 BF 5		Combat at 20 kn E.P.		Combat at 20 kn G.T.		Max speed at 29.5 kn CODLAG	
	Sum. [kW]	Win. [kW]	Sum. [kW]	Win. [kW]	Sum. [kW]	Win. [kW]	Sum. [kW]	Win. [kW]	Sum. [kW]	Win. [kW]	Sum. [kW]	Win. [kW]	Sum. [kW]	Win. [kW]	Sum. [kW]	Win. [kW]
Total power on LV side	1200	1500	1950	2066	2009	2128	2009	2128	2009	2128	2200	2300	2310	2400	2200	2300
Transformer efficiency	0.98															
Total power on HV side	1224	1531	1990	2108	2050	2171	2050	2171	2050	2171	2245	2347	2357	2449	2245	2347
Azimuthal Propeller			1000	1000												
Total ship power on HV side w/o propulsion	1224	1531	2990	3108	2050	2171	2050	2171	2050	2171	2245	2347	2357	2449	2245	2347
Electric propulsion power on HV side			1648	1648	2786	2786	5647	5647	6848	6848	8696	8696			8696	8696
Total ship power on HV side with propulsion	1224	1531	4638	4756	4836	4957	7697	7818	8898	9019	10941	11043	2357	2449	10941	11043
Design margin	10%															
Total ship power w/o propulsion	1347	1684	4937	5067	5041	5174	7902	8035	9103	9236	11165	11277	2593	2694	11165	11277
Running DG	1	1	2	2	2	2	3	3	4	4	4	4	1	1	4	4
Available power	3100	3100	6200	6200	6200	6200	9300	9300	12400	12400	12400	12400	3100	3100	12400	12400
DG load (%)	**43.45**	**54.31**	79.62	81.72	81.30	83.46	84.96	86.40	73.41	74.49	*90.04*	*90.95*	83.64	86.90	*90.04*	*90.95*

TABLE V. EFFICIENCY VALUES

Component	Efficiency
Propulsion electrical motor	0.965
Variable speed drive	0.970
Propulsion transformer	0.990
ESS transformer	0.990
ESS converter	0.970

TABLE VI. RESULTS OF THE PEAK-SHAVING ESS SIZING

	SS4@18kn	SS5@16kn
Capacity	0.9 kWh	1 kWh
Power	600 kW	700 kW
Type	Supercap	Supercap
Weight	5.047 t	5.888 t
Volume	63 m^3	73 m^3
Mean prop. power	6755 kW	7380 kW

margin to take into account future upgrades, it is finally possible to define the total electrical power required by the ship. In this regard, the electric loads balance in Table IV depicts all the data for the considered ship's OCs. It is relevant to notice that electrical propulsion is adopted in the "cruise" OC, in one of the "Combat" (the one depicted with E.P., i.e., Electric Propulsion), in the "silent mode", and in the "preparation for sea". Conversely, the other "Combat" OC (the one depicted with G.T., i.e., Gas Turbine) is based on mechanical propulsion, while in the "Max Speed" one uses the combined power of the gas turbine and the electric motors in CODLAG configuration. Table IV depicts also the amount of DGs that are requested in operation for each OC, as well as their working point (load factor, in percentage). As can be clearly seen, at berth the load on the running DGs is very low, making them operate far from their most efficient working point (data depicted in bold). Conversely, in other OCs the load on the DGs is very high, thus pushing their operation very close to their maximum continuous rating (data depicted in italics). This data is significant for the evaluations made in the following subsections, where the installation of ESSs is evaluated based on two different possible scopes for such subsystems: particularly, peak shaving or zero-emission mode.

C. Peak shaving

The first scope analyzed for the ESS onboard integration is the application of the peak shaving function to the propulsion. Specifically, the objective is the complete compensation of the variations in P_B caused by the waves (Fig. 5). To this aim, the simulated time records of the propulsion power over time (ref. to Section II.A) in different operative conditions have been elaborated through a Matlab script. Being the data referring to the mechanical power at the propeller axis (P_B), a set of hypothetical efficiency values have been defined for the system components, in order to obtain the power values at the main switchboard (Table V). For each analyzed time record, the script calculates the maximum power deviation with respect to the mean value, as well as the values of the area under the deviation curve, providing the two data for each deviation episode. Then, the script identifies the value of both the higest deviation and the highest area under the deviation curve in the time record (c.d. "worst case" deviation). The former is the magnitude of the power (in kW) that must be exchanged with the propulsion system during the deviation and the latter is the required energy (in kWs). These must be delivered by the ESS system for totally compensating the waves' effect. It is relevant to notice that the calculated values are related to a single deviation value, which can either be a positive (increase in power absorbed by propulsion) or a negative (decrease in power absorbed by propulsion) variation. Therefore, it is necessary to apply the following design constraints to proceed with the ESS sizing:

- the ESS must be capable of delivering at least the calculated maximum power regardless of its direction (from the ESS to the propulsion or viceversa);
- the ESS must be capable of exchanging with the propulsion system the required energy also in the case of two consequential "worst case" deviations;
- the ESS must present a sufficient State Of Charge (SOC) margin to allow for the required energy exchanges (both from ESS to propulsion and viceversa).

To ensure the compliance with the first design hypothesis, a safety coefficient equal to 1.5 has been applied to the calculated maximum power. Conversely, to ensure the compliance with the second design hypothesis, the energy required by the "worst case" deviation has been doubled (thus modeling a case in which a maximum energy deviation is followed by another maximum energy deviation of the opposite sign). While such a sizing enables the compensation of a full "worst case" power swing when the ESS is near the 50% SOC value, it leaves only 25% margin from the full (100% SOC) and empty (0% SOC) conditions. Such a limited margin has been deemed not sufficient, taking into account both the variability in the power (Fig. 5) and the need of limiting ESS wear. Therefore, the resulting energy has been doubled again, which leads to a 25% maximum impact of the "worst case" deviation on the ESS SOC value, as well as 37.5% SOC margins if a full "worst case" power swing happens when the ESS is near the 50% SOC value. The resulting energy is then converted in kWh value, to directly provide the required ESS capacity. For what it converns power, the Table V efficiency values have been used to obtain the ESS power from the calculated power data (which was obtained at the main switchboards).

Once the required power and capacity of the ESS have been identified, an evaluation of the most suitable technology for the latter has been done. The decision is made considering only super-capacitors and Li-ion batteries technolgoies, and it is based on the evaluation of the required ESS C-rate (discharge current vs. nominal current) and capacity. The nominal current of the ESS can be easily calculated using its required power and the power system voltage (refer to Fig.8), while the discharge current is proportional to the derivative of the power, obtained form the deviations time records.

Specifically, a high C-rate with low capacity calls for super-capacitors, while the opposite calls for Li-ion batteries. High C-rate and high capacity instead require hybrid ESS systems, integrating both technologies. On the other side, low C-rate and capacity can be met with any technology. If the Matlab script identifies a specific ESS technology, it then calculates an estimation of its weight and volume, based on data obtained from commercial products' datasheets.

The results related to the peak-shaving function are provided in Table VI, together with the mean propulsion power used in the calculation of the power deviations time records. With the proposed sizing, the ESS completely compensates the power variations in the propulsion power, leaving to the onboard DGs only the supply of the mean value. In the worst case of Table VI, which is ship cruising at 16 kn in SS5 (SS5@16kn), the required volume is nearly 75 m^3, while the related weight is nearly 6 t. In the "Cruise at 18 kn, SS4" OC of Table IV (SS4@18kn) the required volume and weight are nearly 63 m^3 and 5 t. Such values guarantee the feasibility of the ESS dedicated to peak shaving, which indeed is sized in the volume and weight limits provided in Section II.C.

In regards to the possible location in the IPES for interfacing such an ESS, there are two possibilities. The first one assumes to connect it to the HV busbars of the system, while the second connects it to the DC links of propulsion drives. In the latter case, the increase in efficiency due to the removal of the transformer and conversion stages would be beneficial to the overall system sizing, but it will oblige to install the peak shaving ESS in the EM room.

There is no need for a dedicated solution for recharging the ESS in this case. Indeed, it is possible to rely on the peak-shaving operation to always keep it charged around 50% of its capacity (value required for correctly providing the peak shaving function), and using ship onboard loads to discharge it when a too high SOC is reached.

D. Zero emission mode

The second scope analyzed for the ESS onboard integration is the ship's zero emission mode navigation. To this aim, the available volume and weight reserve described in Section II.B is used as an input, to identify the highest ESS capacity installable onboard. The power and energy densities used for the ESS for this specific scope are taken from [32], whose data considers both the equipment (converters and energy storage components) and the required support areas (e.g. spaces in front and back of cabinets for inspection and maintenance). The power densities are thus equal to 182 kW/m^3 and 740 W/kg (volumetric and gravimetric respectively), while the energy density depends on the amount of power to be delivered by the ESS. Indeed, energy density takes into account both the converter and the battery volume and weight up to reaching the maximum power, then no more converters are needed and only the battery density can be applied. Consequently, up to the maximum power, the energy density values are 12.9 kWh/m^3 and 52 Wh/kg (volumetric and gravimetric respectively), becoming 53 kWh/m^3 and 100 Wh/kg onwards.

In the zero-emission mode case study, the selected ESS design criteria is the maximization of the ESS powered navigation capability. Thus, the goal is the integration of as much capacity as possible in the available volume and weight limits. To do that, a value for the ESS maximum power has to be defined in order to apply the correct energy density values. Being the zero-emission mode goal the supply of the full propulsion power with energy from the ESS, the required power values have to be retrieved from the data analysis previously made on the propulsion power time records (used for the peak shaving case study), whose results are shown in Table VI. Specifically, the worst-case value of 7380 kW mean power has been chosen as the baseline, and the 700 kW peak power has been added to it to ensure the ESS capability of supplying the entire propulsion power when needed (mean value plus the peak). By adding a suitable sizing margin, a nearly 9 MW required power result is obtained, which is assumed as the sizing value for the ESS conversion system. Therefore, in the available 130 t and 600 m^3 (refer to Section II.B) it becomes possible to install a 9 MW ESS with up to 12.5 MWh capacity. It is relevant to notice that weight constitutes the limiting factor for designing this ESS.

To evaluate the efficacy of such an ESS in enabling the zero-emission mode navigation, it is required to determine both its recharge and discharge times in the relevant OCs of Table IV.

A first option is to use the ESS to feed the ship "at berth", keeping the onboard DGs shut off in an OC where they have a very low load factor. The required power results compatible with the ESS sizing. In the hypothesis of having the ESS fully loaded, the loads can be fed for almost 7 and a half hours (12.5 MWh / 1684 kW = 7.42 hours).

A second option is to sail with the DGs completely shut off, relying only on the ESS stored energy. Being the rated power of the ESS equal to 9 MW, the only conditions in which this is applicable are "preparation for sea" and "cruise" at both 12 and 15 kn speed. The third OC (cruise at 15 kn) provides the greatest power absorption in wintertime (8035 kW). With this load level, the fully charged ESS discharges in just over 15 hours and a half (12.5 MWh / 8035 kW = 15,557 hours), while in the other OCs it will last for a longer time.

A final option is to use the ESS to supply power to the loads in all the OCs that require the DGs to operate above 87% load factor (i.e., maximum efficiency point). In such a case, the DGs load can be locked at their optimum load factor, and the ESS can be used to supply the remaining power. Such an operation is not a zero-emission mode one, but it is nonetheless capable of reducing the fuel consumption of the ship. To evaluate such a case, the "combat at 20 kn, E.P. winter" condition is selected, which means a ship in combat role, navigating at 20 kn using electric propulsion system only. In such an OC, 122 kW would be needed from the ESS to keep the DGs at 87% load factor. The required power is very low in respect to the ESS sizing, and makes it possible to keep operations for more than 100

hours (12.5 MW / 122 kW = 102.46 hours) assuming a fully charged ESS at the start of the navigation.

In regards to the possible location in the IPES for interfacing the ESS, the only viable solution is to divide it into two equal sections (each half the power/capacity), to be installed on the HV busbars. Such a choice allows obtaining redundancy and enables the ESS recharge from either the DGs, the shore interface, or the propulsion system. The latter possibility is made possible by using reversible variable frequency drives in a shaft generator configuration.

For what concerns the ESS recharge, the best solution is to do it through the shore power interface, thus when the ship is moored. This is because it is cheaper to buy energy from the shore network than to produce it onboard with the DGs. However, there may be situations in which there is no shore connection available. Therefore, the onboard DGs can be used to recharge the ESS, using the additional load to reach their optimal load factor (here set at 87%) n the "at berth" OC. Thus, 1350 kW would be available in summer and 1013 kW in winter, which respectively makes it possible to recharge the ESS from empty to full in about 9 and a half hours in the first case (12.5 MWh /1350 kW = 9.26 hours), and 12 and a half hours in the second case. Conversely, the other OCs already present high DGs load factors, making it available a very low power for the ESS recharge, and can therefore be neglected. The only exception is the "cruise at 18 kn with SS4" OC, (421 and 388 kW respectively in summer and winter), where for each hour of navigation it is possible to recharge about 0.4 MWh of battery.

V. Conclusions

The design of a modular multirole frigate with IPES offers significant advantages over traditional naval platforms. The modular architecture provides greater flexibility, enabling the vessel to perform a wider range of missions. This is particularly valuable in today's rapidly evolving security environment, where vessels must be capable of adapting to new threats and operative environments.

In this work, a new design has been proposed to test the feasibility of multiple configurations of IPES. First, the implementation of peak shaving technology based on supercapacitors resulted in a compact and lightweight solution, allowing the avoidance of fluctuating loads on diesel generators, which can improve reliability and reduce maintenance costs. Thus, this solution is highly recommended for such kinds of naval platforms based on CODLAG.

In addition to these benefits, the frigate's IPES allows the ship to operate in zero-emission mode while in port or during maneuvers, which has a positive impact on local pollution in a sensible area nearby the coast. This is becoming increasingly important in the maritime industry, where there is growing pressure to reduce greenhouse gas emissions and protect marine ecosystems. By minimizing its environmental footprint, the frigate can not only reduce the manning costs but also enhance the Navy's reputation as a responsible and sustainable actor in the maritime domain.

To further improve efficiency, it is recommended to avoid using multiple generators at low loads when in port, and, instead, opt for shore connection or intermittently activating a single generator at optimal load to charge the batteries. This can help reduce fuel consumption and emissions, as well as prolong the life of the generators.

Finally, future developments may include using batteries to operate in silent mode at low speeds for a certain time. This might be useful for several missions such as anti-submarine warfare. Besides, to improve the efficiency of the electric generation plant when multiple generators are active, the load of each generator might be optimized to minimize fuel consumption. These measures can help enhance the frigate's operational capabilities while reducing its environmental impact and overall operating costs. Additional future work may also include comparing the hybrid propelled solution here analyzed with a full electric one. However, this will need a complete redesign of the case study ship to correctly evaluate available space and volume, which can significantly vary as demonstrated in [34]. Finally, real measurement data can be exploited to further detail the analyses here depicted, introducing emissions evaluations to possibly optimize the ESS sizing.

References

[1] S. K. Chen and S. H. Chen, "Onboard energy management for ship auxiliary systems: a review," Renewable and Sustainable Energy Reviews, vol. 45, pp. 225-237, May 2015.

[2] R. Geertsma, J. Vollbrandt, R. Negenborn, K. Visser and H. Hopman, "A quantitative comparison of hybrid diesel-electric and gas-turbine-electric propulsion for future frigates," 2017 IEEE Electric Ship Technologies Symposium (ESTS), Arlington, VA, USA, 2017, pp. 451-458, doi: 10.1109/ESTS.2017.8069321.

[3] K. E. Carballo, A. J. Jones, and T. J. Troutman, "Modular Shipbuilding: An Innovative Approach to Naval Ship Design and Construction," in Naval Engineers Journal, vol. 123, no. 1, pp. 67-77, Jan. 2011, doi: 10.1111/j.1559-3584.2011.00327.x.

[4] J. Witsen and M. Oosterveld, "Advanced modularization in shipbuilding: designing a containerized module," in Procedia CIRP, vol. 52, pp. 17-22, 2016, doi: 10.1016/j.procir.2016.08.004.

[5] M. Majewski, "Flexible and modular ship design in the context of changing operational requirements," in Scientific Journals of the Maritime University of Szczecin, vol. 47, no. 119, pp. 24-30, 2016, doi: 10.17402/154.

[6] R. J. Yager and A. L. Hall, "Emerging Technologies for Naval and 37, no. 1, pp. 60-68, Spring 2018, doi: 10.1109/MTS.2018.2798173.

[7] A. Vicenzutti, G. Sulligoi, V. Bucci, S. Bertagna, M. Cataneo and P. Borghese, "Naval Smart Grid Preliminary Integration onboard Electric Ships," 2021 IEEE Electric Ship Technologies Symposium (ESTS), Arlington, VA, USA, 2021, pp. 1-7, doi: 10.1109/ESTS49166.2021.9512326.

[8] D. Brefort, C. Shields, A. Habben Jansen, E. Duchateau, R. Pawling, K. Droste, T. Jasper, M. Sypniewski, C. Goodrum, M. A. Parsons, M. Y. Kara, M. Roth, D. J. Singer, D. Andrews, H. Hopman, A. Brown, and A. A. Kana, "An architectural framework for distributed naval ship systems," Ocean Eng., vol. 147, pp. 375-385, 2018, doi: 10.1016/j.oceaneng.2017.10.028.

[9] D. Zhao, D. Li, X. Li, and Y. Zhang, "A review of integrated power and propulsion systems for naval ships," Journal of Marine Science and Technology, vol. 25, no. 1, pp. 1-12, Jan. 2020.

[10] H. Zhao, S. Zhao, X. Zhang, and B. Jiang, "Energy management strategies for a hybrid energy storage system in a small electric vessel,"

IEEE Transactions on Industrial Electronics, vol. 65, no. 6, pp. 4792-4802, Jun. 2018.

[11] L. Braidotti, S. Bertagna, R. Rappoccio, S. Utzeri, V. Bucci, and A. Marinò, "On the inconsistency and revision of Carbon Intensity Indicator for cruise ships," Transportation Research Part D: Transport and Environment, vol. 2023, in press.

[12] G. Trincas, F. Mauro, L. Braidotti and V. Bucci "Handling the Path from Concept to Preliminary Ship Design", Proceedings of the 13th International Marine Design Conference, IMDC 2018, Kujala & Lu ed., CRC Press, Helsinki, vol. 1, pp 181-191.

[13] M. Mauro, F. Francesco, L. Braidotti, and G. Trincas, "Determination of an optimal fleet for a CNG transportation scenario in the Mediterranean Sea," Brodogradnja, vol. 70, no. 3, pp. 1-23, 2019.

[14] F. Mauro, L. Braidotti, and G. Trincas, "A Model for Intact and Damage Stability Evaluation of CNG Ships during the Concept Design Stage," Journal of Marine Science and Engineering, vol. 7, no. 12, p. 450, Dec. 2019, doi: 10.3390/jmse7120450.

[15] S. Kunz, M. Grossmann, M. Schönberger, and S. Wartzack, "Innovative production techniques for shipbuilding: a review," in Journal of Ship Production and Design, vol. 37, no. 3, pp. 167-179, 2021, doi: 10.5957/JSPD.210012.

[16] M. Merklein, J. K. Spatzier and A. Dittrich, "Additive manufacturing of composite structures," in CIRP Annals, vol. 69, no. 1, pp. 451-474, 2020, doi: 10.1016/j.cirp.2020.03.050.

[17] Y. Cheng, X. Lu and F. Yang, "3D printing of shipbuilding materials and structures: A review," in Journal of Ship Production and Design, vol. 36, no. 1, pp. 1-13, 2020, doi: 10.5957/JSPD.180021.

[18] L. Braidotti, S. Bertagna, A. Marinò, D. Bosich, V. Bucci and G. Sulligoi, "An Application of Modular Design in the Refitting of a Hybrid-electric Propelled Training Ship," 2020 AEIT International Annual Conference (AEIT), Catania, Italy, 2020, pp. 1-6, doi: 10.23919/AEIT50178.2020.9241114.

[19] M. J. Flynn, M. C. Goldsberry, T. M. Urbina and B. A. Zinnen, "NATO Generic Open Architecture (NGOA) and Data Format Standards for Interoperable Military Modular Payloads," in Journal of Marine Science and Engineering, vol. 6, no. 1, p. 19, 2018, doi: 10.3390/jmse6010019.

[20] B. K. Rasmussen, "StanFlex-Modular Mission Payload System," in The Journal of Defense Software Engineering, vol. 22, no. 2, pp. 12-16, 2009.

[21] T. M. Urbina, M. J. Flynn and M. C. Goldsberry, "Modular Mission Payload (MMP): A Systems Approach to Building the Future Naval Force," in Journal of Marine Science and Engineering, vol. 4, no. 3, pp. 50-68, 2016, doi: 10.3390/jmse4030050.

[22] P. G. Ivankovic, M. H. G. Peters and J. W. S. Hearle, "Marine composites for modular shipbuilding," in Composites Science and Technology, vol. 63, no. 6, pp. 821-826, 2003, doi: 10.1016/S0266-3538(02)00213-5.

[23] C. R. Baxter, "The development of modular warships," in Naval Engineers Journal, vol. 126, no. 1, pp. 107-116, Jan. 2014, doi: 10.1111/nejo.12047.

[24] J. J. Dackermann, "Modularity in naval ship design," in Journal of Ship Production and Design, vol. 31, no. 2, pp. 91-98, 2015, doi: 10.5957/JSPD.31.2.140004.

[25] G. Avlonitis and G. Kavarnos, "Containerization in ship design," in Ocean Engineering, vol. 158, pp. 43-53, 2018, doi: 10.1016/j.oceaneng.2018.04.001.

[26] M. Przerwa, R. Szczebiot and A. Werbinska-Wojciechowska, "Review of Modularity in Naval Ships Design and Operation," in TransNav: International Journal on Marine Navigation and Safety of Sea Transportation, vol. 13, no. 4, pp. 811-816, 2019, doi: 10.12716/1001.13.04.24.

[27] J.A. Malone, D.E. Litle and M. Allman, "Effects of Hull Foulants and Cleaning/Coating Practices on Ship Performance and Economics", Trans. SNAME, vol. 88, 1980.

[28] A. R. J. M. Lloyd, Seakeeping – Ship Behaviour in Rough Weather. Ellis Horwood, 1989.

[29] W. J. Pierson and L. Moskowitz, "A proposed spectral form for fully developed wind seas based on the similarity theory of S. A. Kitaigorodskii," J. Geophys. Res., vol. 69, no. 24, pp. 5181-5190, 1964.

[30] S. Liu and A. Papanikolaou, "Regression analysis of experimental data for added resistance in waves of arbitrary heading and development of a semi-empirical formula," Ocean Eng., vol. 206, pp. 107357, 2020, doi: 10.1016/j.oceaneng.2020.107357.

[31] T. Fujiwara and T. Nimura, "New Estimation Method of Wind Forces Acting On Ships On the Basis of Mathematical Model," presented at the The Fifteenth International Offshore and Polar Engineering Conference, Seoul, Korea, Jun. 2005.

[32] I. A. Voitkunsky, "Resistance of Sailing Ships" (in Russian), Sudostroyenie Publishing House, Leningrad, 1988, ISBN 5-7355-0032-5.

[33] G. Sulligoi, G. Trincas, A. Vicenzutti, L. Braidotti and M. Cataneo, "Concept Design Methodology to Enable Naval Smart Grid onboard Electric Ships," 2021 IEEE Electric Ship Technologies Symposium (ESTS), Arlington, VA, USA, 2021, pp. 1-9, doi: 10.1109/ESTS49166.2021.9512322.

[34] A. Vicenzutti, G. Trincas, V. Bucci, G. Sulligoi and G. Lipardi, "Early-Stage design methodology for a multirole electric propelled surface combatant ship," 2019 IEEE Electric Ship Technologies Symposium (ESTS), Washington, DC, USA, 2019, pp. 97-105